

We are IntechOpen, the world's leading publisher of Open Access books Built by scientists, for scientists

6,900

Open access books available

186,000

International authors and editors

200M

Downloads

Our authors are among the

154

Countries delivered to

TOP 1%

most cited scientists

12.2%

Contributors from top 500 universities



WEB OF SCIENCE™

Selection of our books indexed in the Book Citation Index
in Web of Science™ Core Collection (BKCI)

Interested in publishing with us?
Contact book.department@intechopen.com

Numbers displayed above are based on latest data collected.
For more information visit www.intechopen.com



Precision Dimensional Metrology based on a Femtosecond Pulse Laser

Jonghan Jin^{1,2} and Seung-Woo Kim²

¹*Center for Length and Time, Division of Physical Metrology, Korea Research Institute of Standards and Science (KRISS)*

²*Ultrafast Optics for Ultraprecision Technology Group, KAIST Republic of Korea*

1. Introduction

Metre is defined as the path traveled by light in the vacuum during the time interval of $1/299\,792\,458$ s. The optical interferometer allows a direct realization of metre because it obtains the displacement based on wavelength of a light source in use which is corresponding to the period of interference signal. Due to the periodicity of interference signal, the distance can be determined by accumulating the phase continuously to avoid the 2π ambiguity problem while moving the target. Conventional laser interferometer systems have been adopted this relative displacement measurement technique for simple layout and high measurement accuracy.

Recently the use of femtosecond pulse lasers (fs pulse laser) has been exploded because of its wide spectral bandwidth, short pulse duration, high frequency stability and ultra-strong peak power in precision spectroscopy, time-resolved measurement, and micro/nano fabrication. A fs pulse laser has more than 10^5 longitudinal modes in the wide spectral bandwidth of several hundred nm in wavelength. The longitudinal modes of a fs pulse laser, the optical comb can be described by two measurable parameters; repetition rate and carrier-offset frequency. A repetition rate, equal spacing between longitudinal modes is determined by cavity length, and a carrier-offset frequency is caused by dispersion in the cavity. Under stabilization of the repetition rate and a carrier-offset frequency, longitudinal modes are able to be employed as a scale on the optical frequency ruler with the traceability to the frequency standard, cesium atomic clock.

Optical frequency generators were suggested and realized to generate a desired well-defined wavelength by locking an external tunable working laser to a wanted longitudinal mode of the optical comb or extracting a frequency component directly from the optical comb with optical filtering and amplification stages. Optical frequency generators can be used as a novel light source for precision dimensional metrology due to wide optical frequency selection with the high frequency stability.

In this chapter, the basic principles of a fs pulse laser and optical frequency generators will be introduced. And novel measurement techniques using optical frequency generators will be described in standard calibration task and absolute distance measurement for both fundamental research and industrial use.

Source: *Advances in Solid-State Lasers: Development and Applications*, Book edited by: Mikhail Grishin, ISBN 978-953-7619-80-0, pp. 630, February 2010, INTECH, Croatia, downloaded from SCIYO.COM

2. Basic principles of precision dimensional metrology

2.1 Optical comb of a fs pulse laser

Precision measurement of optical frequency in the range of several hundred THz has lots of practical difficulties because the bandwidth of photo-detectors only can reach up to several GHz. Simply it can be determined by beat notes with well-known optical frequencies like absorption lines of atoms or molecules in the radio frequency regime, which are detectable. And the other method, frequency chain, was realized which could connect from radio frequency regime to optical frequency regime with numerous laser sources and radio /micro frequency generators, which were stabilized and locked to the frequency standard by beat signals of them in series. The construction and arrangement of components for this frequency chain should be changed according to the optical frequency we want to measure. That makes it is not attractive as general optical frequency measuring technique in terms of efficiency and practicality.

The advent of a fs pulse laser could open the new era for precision optical frequency metrology. The absolute optical frequency measurement technique was suggested based on the optical comb of a fs pulse laser, which could emit a pulse train using a mode-locking technique. Since the optical comb has lots of optical frequency modes, it can be employed as a scale on the frequency ruler under stabilization. Prof. Hänsch in MPQ suggested this idea, and verified the maintenance of phase coherence between frequency modes of the optical comb experimentally. However, it could not be used because the spectral bandwidth is not wide enough for covering an octave. Dr. Hall in NIST realized the wide-spectral optical comb firstly with the aid of a photonic crystal fiber, which could induce the non-linear effect highly. That allows a direct optical frequency measurement with the traceability to the frequency standard. And it also has been used in the field of precision spectroscopy.

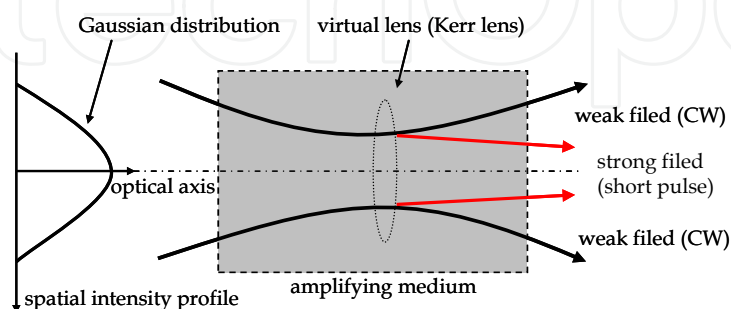
Laser based on the optical cavity can have lots of longitudinal modes with the frequency mode spacing of $c/2L_c$, where c is speed of light and L_c represents the length of optical cavity. When spectral bandwidth of an amplifying medium is broad enough to have several longitudinal modes, it can be operated as a multi-mode emission. Typical a monochromatic laser is designed to produce a single frequency by shortening length of the optical cavity, which leads wide frequency mode spacing. In the case of a fs pulse laser, the Ti:Sapphire has very wide emission bandwidth of 650 to 1100 nm with the absorption bandwidth of 400 to 600 nm. Even if the spectral bandwidth is only 50 nm with frequency mode spacing of 80 MHz at a center wavelength of 800 nm, number of longitudinal modes can be reached to 3×10^5 . Though the modes are oscillating independently, the phases of whole modes can be made same based on strong non-linear effect, Kerr lens effect.

Mode-locking can be achieved by Kerr lens effect in the amplifying medium with a slit. When strong light propagates into a medium, Kerr lens effect can lead change of refractive index of the medium according to the optical intensity of an incident light. Therefore, the refractive index of the medium, n , can be expressed as

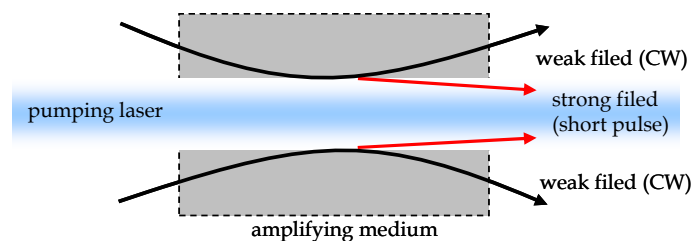
$$n = n_0 + n_2 \cdot I \quad (2-1)$$

where n_0 is the linear refractive index, n_2 is the second-order nonlinear refractive index, and I is intensity of the incident light. Since the plane wave has Gaussian-shaped intensity profile spatially, the high intensity area near an optical axis suffers the high refractive index relatively. That makes self-focusing of the strong light as shown in figure 2-1(a). In order to generate a pulse train, the difference gains for continuous waves and pulsed waves are

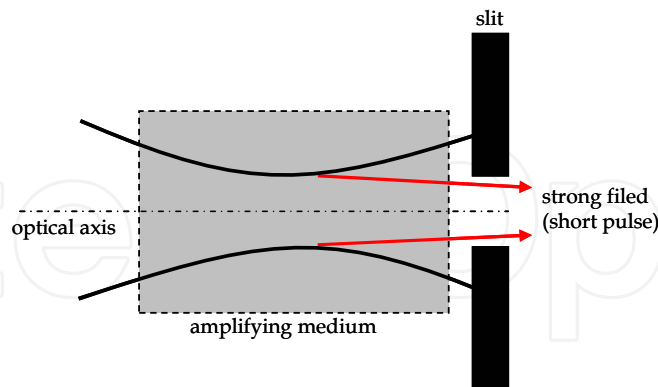
induced by two methods; One is the adjusting the beam size of a pumping laser to have more gain in the only high intensity area as shown in figure 2-1 (b). The other is removal of the continuous wave by a slit in figure 2-1 (c). That is, the short pulse has stronger optical intensity than a continuous wave, which is caused by Kerr lens effect in the amplifying medium. By designing the optimal cavity the short pulse will be activate with high gain, and the continuous light will be suppressed. In the begging of generation of a short pulse, the small mounts of shock or impact should be needed to give intensity variation for inducing non-linear effect efficiently.



(a) Self-focusing of Kerr lens effect



(b) Generation of pulses by adjusting the pumping beam size (soft-aperture)



(c) Generation of pulses with a slit (hard-aperture)

Fig. 2-1. Basics of Mode-locking; Kerr lens effects and cavity design for introducing differential gain

Figure 2-2 shows the generation of pulse train when the modes are phase-locked according to the number of participating frequency modes. The pulse duration can be shortened by employing numerous frequency modes in the mode-locking process, it can be achieved several fs or less in time domain. Typically a commercialized Ti:Sapphire fs pulse laser has

the spectral bandwidth of more than 100 nm in wavelength (There are approximately 10^5 or more longitudinal modes.) and the pulse duration of less than 10 fs.

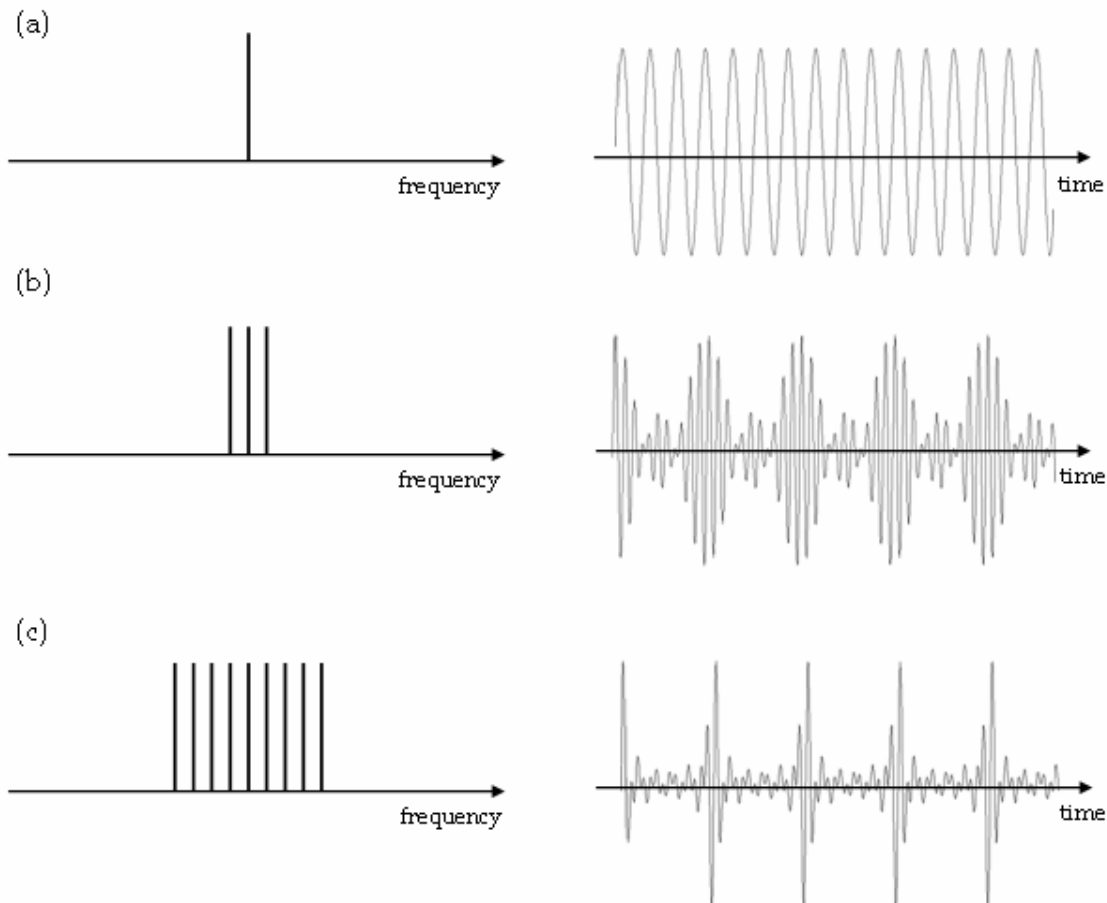
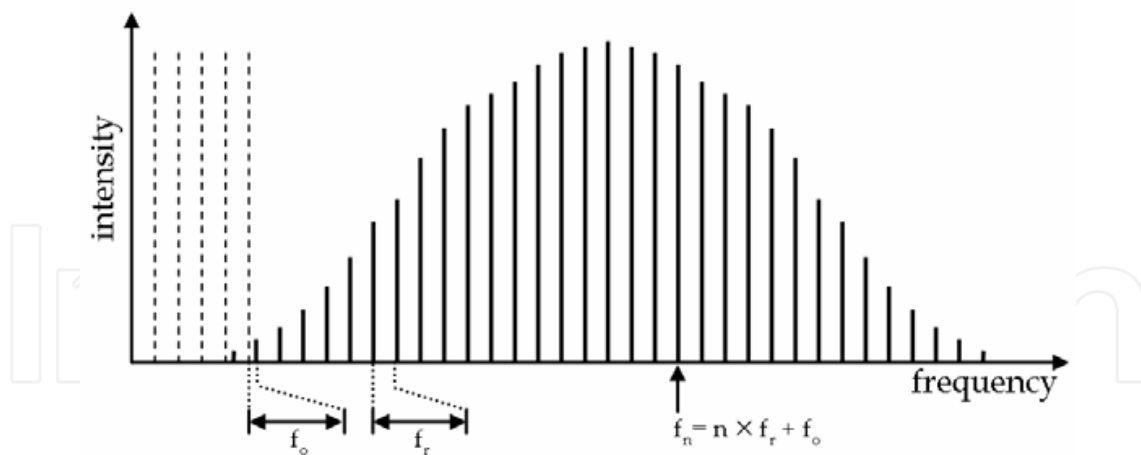


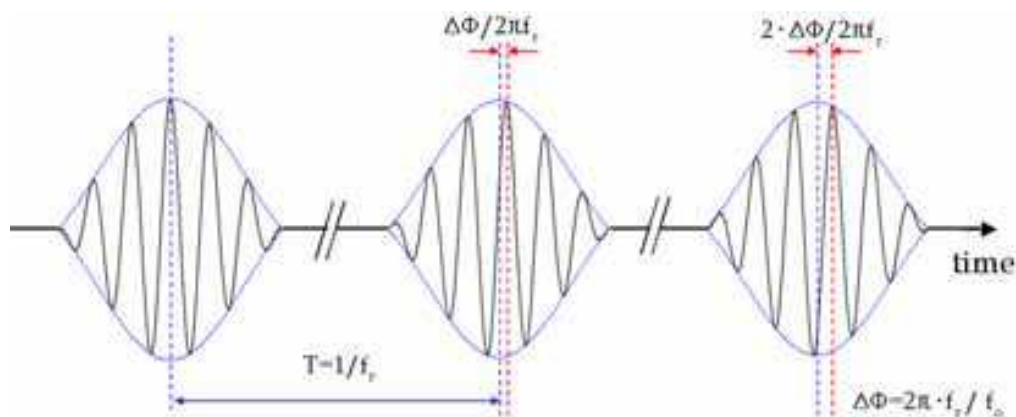
Fig. 2-2. Relationship between frequency and time-domain; (a) single frequency, (b) three frequencies, (c) nine frequencies with same initial phase values.

Figure 2-3(a) shows the optical comb, which can be described by repetition rate, f_r and carrier-offset frequency, f_o . Repetition rate, mode spacing in the frequency domain, can be monitored by photo-detector easily, and adjusted by translating of the end mirror of the cavity to change the cavity length. The carrier-offset frequency caused by dispersion in the cavity is defined as frequency shift or offset of the whole optical comb from the zero in the frequency domain. It can be measured by a self-referencing f - $2f$ interferometer, and controlled by prism pairs, diffraction gratings, or chirped mirrors in order to compensate the dispersion. Figure 2-3(b) shows pulse train of a fs pulse laser in time domain. The time interval of pulses, T , is defined by the reciprocal of the repetition rate, f_r . The shift of the carrier signal from the envelope peak because of the pulse-to-pulse phase shift, $\Delta\Phi$, is caused by carrier-offset frequency, f_o .

Even if the optical comb has a wide spectral bandwidth, that is not sufficient for f - $2f$ interferometer, which is needed the octave-spanned spectrum. The fs pulse laser delivers into a photonic crystal fiber for octave-spanning, then both frequency, f , and doubled frequency, $2f$, components are obtained. The broadening of the spectrum can be occurred by non-linear phenomena such as four-wave mixing generation, self phase modulation, and stimulated Raman scattering. The broadened spectrum divided into two parts, low



(a) Optical comb of a fs pulse laser; repetition rate (f_r), carrier-offset frequency (f_0), n^{th} longitudinal mode (f_n)



(b) Pulse train of a fs pulse laser; time interval between pulses (T), pulse-to-pulse phase shift ($\Delta\Phi$)

Fig. 2-3. Optical comb of a fs pulse laser in spectral domain and time domain.

frequency part (f) and high frequency part ($2f$) by a dichromatic mirror. Here, the n^{th} frequency of longitudinal modes, f_n , can be expressed by the simple equation of

$$f_n = n \times f_r + f_0 \tag{2-2}$$

The low frequency part (f_n) is frequency-doubled, $2f_n$, by a second harmonic generator, then makes the beat note with high frequency part (f_{2n}). It gives the carrier-offset frequency, f_0 , which is given as

$$2f_n - f_{2n} = 2(n \times f_r + f_0) - (2n \times f_r + f_0) = f_0 \tag{2-3}$$

Therefore, all longitudinal modes of the optical comb can be stabilized precisely by locking two parameters, f_r and f_0 , to the atomic clock in the radio frequency regime. For this locking process, phase-locked loop (PLL) was adopted. PLL generates periodic output signal with different duty ratio, which depends on the frequency and phase differences of two inputs based on XOR logic. The periodic output signal can convert to DC signal by a low pass filter, then the DC signal acts as input of voltage-controlled oscillator to coincide frequencies and

phases of two inputs. Figure 2-4 shows a schematic of control loop for repetition rate and carrier-offset frequency stabilization of the fs pulse laser.

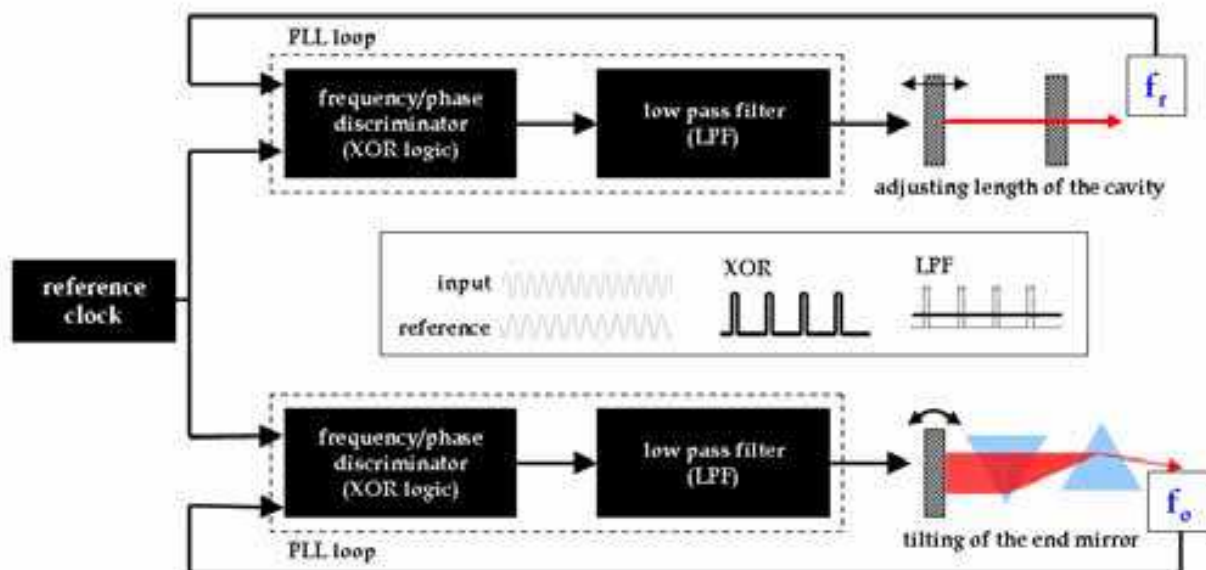


Fig. 2-4. Schematic of control loop for fs pulse laser stabilization

Since the optical frequency of more than several hundreds THz is too fast to detect directly, the optical comb has attractive advantages in the field of ultra-precision optical frequency measurement. Since the optical comb acts as a precision scale on an optical frequency ruler, the optical frequency, f can be obtained by simply adding or subtracting the beat note, f_b to the nearest frequency mode, f_n . It can be given as

$$f = f_n \pm f_b = (n \cdot f_r + f_o) \pm f_b \quad (2-4)$$

By modulating repetition rate or carrier-offset frequency slightly, the sign of beat note can be determined. And more highly accurate optical frequency measurements will be achieved with the advent of ultra-stable optical clocks in the near future.

2.2 Realization of optical frequency generators

Optical frequency generator is an ultra-stable tunable light source, which is able to produce or to extract desired optical frequencies (wavelengths) from the optical comb of a fs pulse laser. Because optical interferometer allows direct realization of length standard based on the wavelength of a light source in use, one or more well-defined wavelengths should be secured. Typically the stabilized wavelength can be obtained by absorption lines or transition lines of atoms or molecules. For multi-wavelength applications it will be a complicated system with different stabilities at desired wavelengths. However, optical frequency generator is a simple solution to produce numerous well-defined wavelengths which are traceable to an unique reference clock of time standard.

In order to realize the optical frequency generator, Extra-cavity laser diode (ECLD), one of useful light sources for wide wavelength tuning range of ~ 20 nm with narrow line-width, was adopted as a working laser as shown in figure 2-5. However, it is not proper to apply it for precision dimensional metrology due to ignorance of absolute frequency and unsatisfied frequency stability. By integrating the ECLD with the stabilized optical comb, the optical

frequency generator can be realized as shown in figure 2-6. The ECLD can tune the wavelength easily by tilting the end mirror using a DC-motor and a PZT coarsely. The input current and the temperature control of the ECLD allow precise wavelength tuning with the resolution of several Hz.

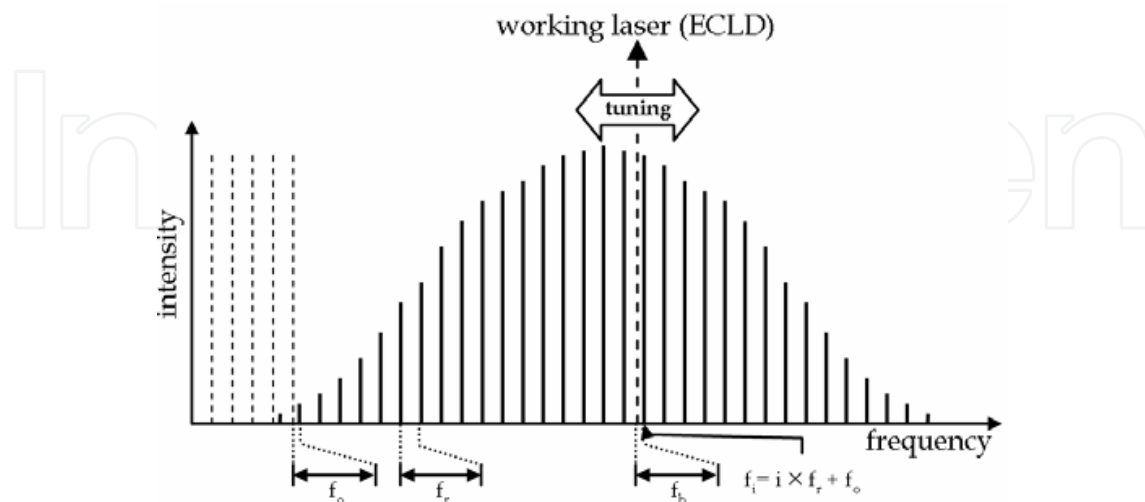


Fig. 2-5. Basic concept of an optical frequency generator with a working laser

A working laser, ECLD consists of a diode laser and an extra cavity; One side of diode laser was anti-reflection coated, the other side was high reflective coated for the end mirror of an external cavity. The diode laser is temperature controlled with the resolution of less than 1 mK by an attached thermometer and an active cooling pad. The light emitted from the diode laser is collimated and goes to the diffraction grating. Then the diffracted light is propagated to the end mirror of external cavity, which can be angle-adjustable using attached DC motor and PZT. Since the angle of the end mirror can be read by an angle sensor precisely, the wavelength of ECLD can be tuned with the resolution of less than 0.02 nm.

The wavelength tuning of ECLD by the DC motor can achieve the resolution of 0.02 nm with speed of 8 nm/s in the range of 765 to 781 nm. The wavelength can be tuned precisely using PZT within only the range of 0.15 nm (75 GHz) due to the short travel of PZT. This control loop has the bandwidth of several hundreds Hz, which is limited by resonance frequency of the mechanical tilting end mirror.

When a target wavelength is inputted, the wavelength of a working laser is tuned coarsely by DC motor and PZT. Because of the short tuning range of PZT, it should be within the small deviation from a target wavelength, 0.15 nm. After that the fine tuning will be done by modulating the input current under temperature stabilization according to the beat note between a nearest comb mode and ECLD, f_b . The current control can be achieve the control rate of 1 MHz. Since the wave-meter has the measurement uncertainty of 30 MHz, it can determine only integer part (i) of the nearest comb mode (f_i) with known values of repetition rate (f_r) and carrier-offset frequency (f_0). And the control loop operates based on a phase-locked loop (PLL) technique which is referred to an atomic clock. The output power of the optical frequency generator is 5 to 20 mW with linewidth of less than 300 kHz at 50 ms, which is corresponding to the coherence length of more than 1 km.

Figure 2-7 shows coarse wavelength tuning performance using the DC motor and the PZT attached on the ECLD. The tuning range is from 775 nm to 775.00025 nm with the step of 0.00005 nm in vacuum wavelength. The frequency stability at each step is about 10^{-8} , which

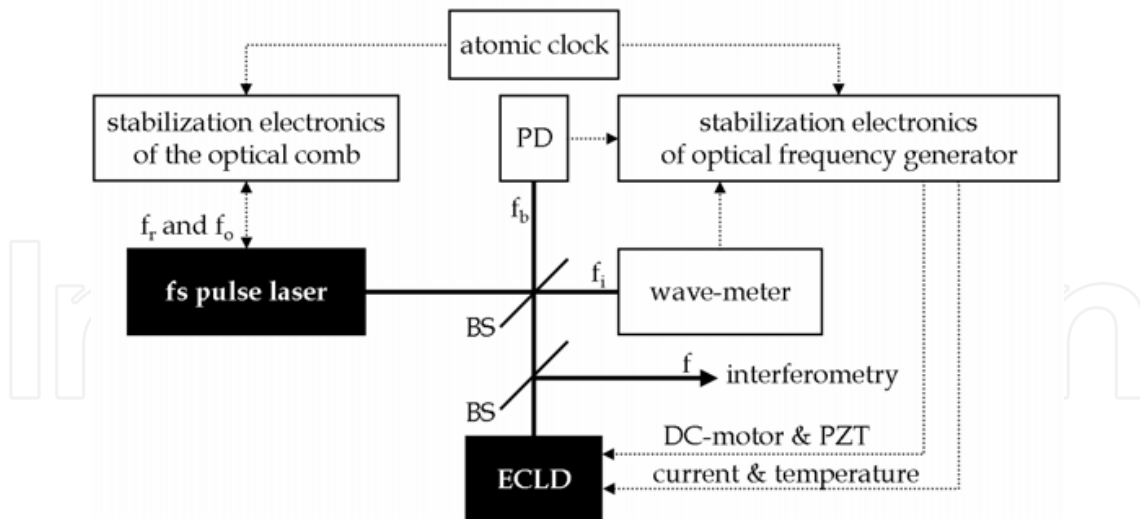


Fig. 2-6. Schematic of the optical frequency generator with wavelength tunable light source; PD(photo-detector), solid lines for optical delivery and dotted lines for electric signals

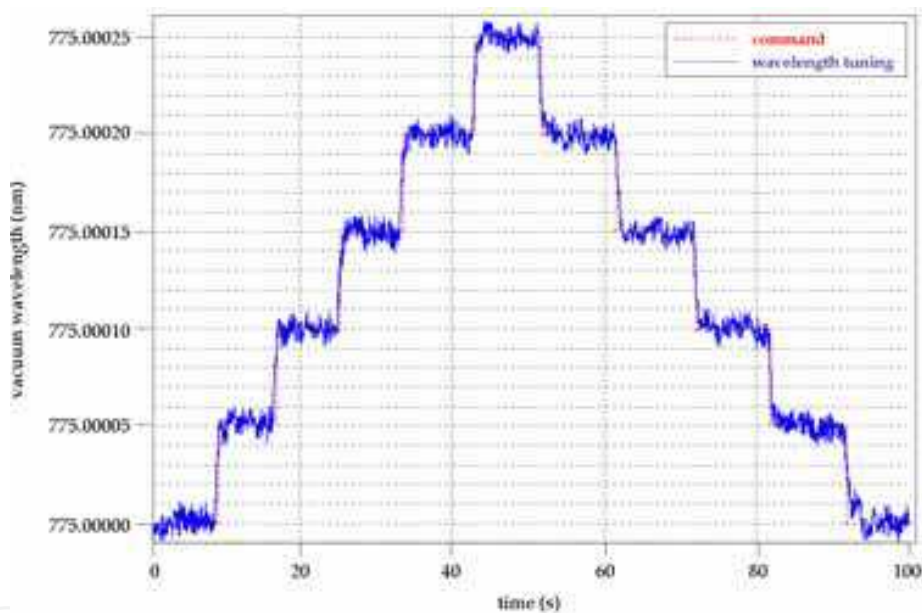


Fig. 2-7. Coarse wavelength tuning performance of an optical frequency generator; solid line is wavelength of ECLD and dotted line is command for coarse tuning.

is frequency deviation of 4 MHz (peak-to-valley value) at 387 THz in frequency. This coarse tuning can be done within 1 s at each step. And then finally the stability of wavelength can be achieved to 1.3×10^{-10} at 10 s by locking beat note, f_b to the rubidium reference clock. This type of the optical frequency generator, however, has a drawback which is a degradation of frequency stability due to the mechanical control and resonance of the ECLD. The other trial for obtaining better frequency stability is the direct extraction of desired wavelengths from the optical comb as shown in figure 2-8. The extraction process consists of coarse and fine filtering. For coarse extraction, the wide tuning range is necessary to cover the whole spectral range of a fs pulse laser even if it has relatively broad filtering bandwidth. In order to extract a single mode from the optical comb, fine filtering should

have the filtering bandwidth smaller than a repetition rate. The optical power of the extracted mode is very weak, thus it should be amplified for applications.

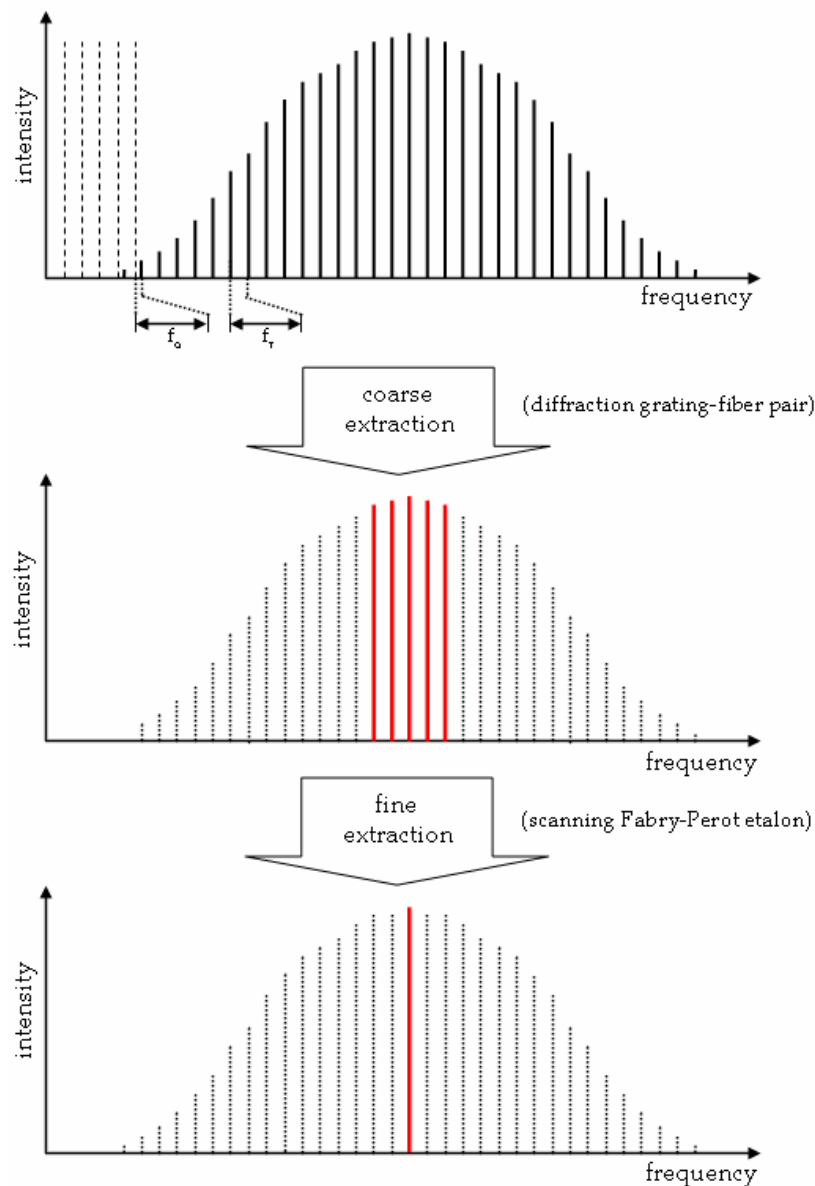


Fig. 2-8. Basic concept of optical frequency generator based on one-mode extraction; dotted longitudinal modes filtered out.

Figure 2-9 shows the optical layout and a schematic of the control system. The desired wavelength can be extracted by diffraction grating-fiber pair coarsely and scanning Fabry-Perot etalon (FPE) finely. By tilting the angle of the diffraction grating or translating the focusing lens of optical fiber, the optical comb can be filtered roughly with the resolution of several hundreds MHz. The FPE can select a desired mode by adjusting the length of the etalon with the resolution of several tens MHz, which is enough to resolve an individual comb mode. However, the selected mode is too weak to detect directly, consequently the injection locking technique is adopted for optical amplification. Optical power of ~ 10 mW can be achieved with the amplification factor of 10^6 . To evaluate the frequency stability, the selected mode is frequency-shifted by AOM and then interfered with the original optical comb.

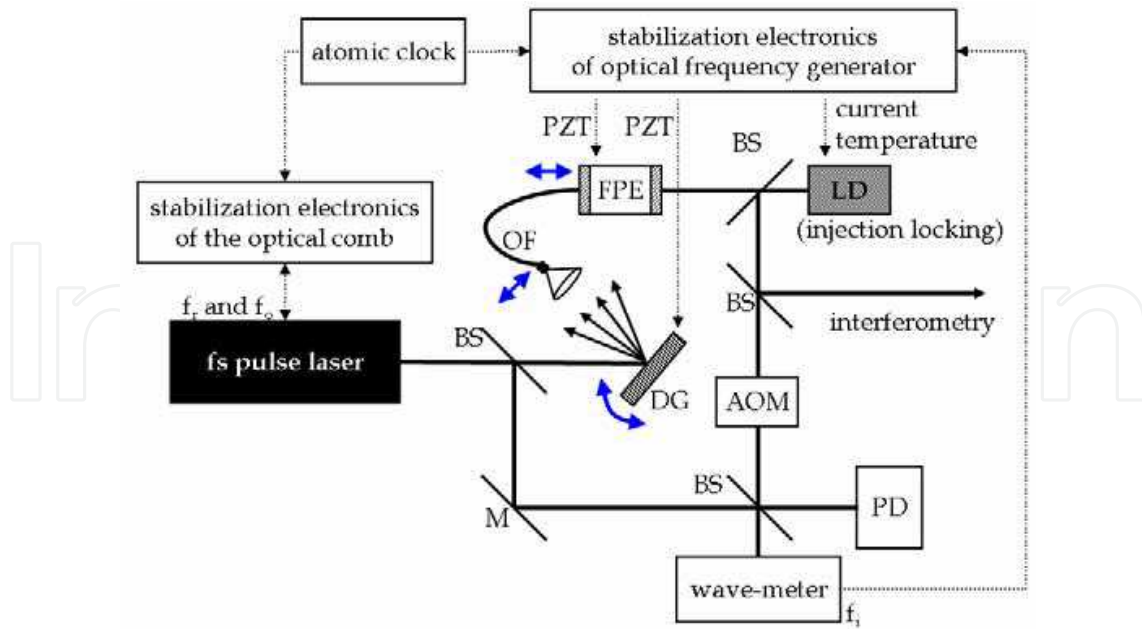


Fig. 2-9. Schematics of optical frequency generator based on direct extraction; DG(diffraction grating), OF(optical fiber), BS(beam splitter), M(mirror), AOM(acoustic-optic modulator), FPE(Fabry-Perot etalon), PD(photo-detector), LD(laser diode)

	optical frequency generator with a working laser	optical frequency generator based on a mode extraction
tuning range	~ 20 nm	10 ~ 15 nm
wavelength stability	$10^{-10} \sim 10^{-11}$	10^{-12} (same as the reference clock)
optical power	20 mW	10 mW
control time	< 1 s	< 1 s

Table 2-1. Summary of the performance of optical frequency generators

Figure 2-10 shows the tuning performance with the step of 5 mode spacing of ~ 400 MHz at a repetition rate of 80 MHz. The angle of diffraction grating was adjusted near 373221494.8 MHz, and then the length of the Fabry-Perot etalon was controlled precisely. The frequency

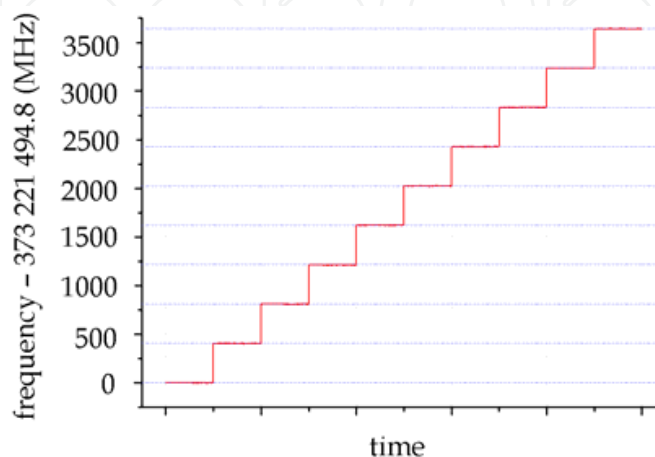


Fig. 2-10. Tuning performance of optical frequency generator based on one-mode extraction

stability of an extracted mode can be achieved 10^{-12} at 10 s, which is the same level as the reference clock. Table 2-1 shows the summary of the performance of optical frequency generators.

2.3 Basic principles of optical interferometer

Optical interference is the superposition of two or more lights that result in a new pattern, which depends on the optical path differences of rays. Since the interference pattern is very sensitive to the optical path difference, the displacement can be determined with sub-wavelength resolution. Figure 2-11(a) shows Michelson's interferometer, the most well-known optical layout, used in precision dimensional metrology. Light emitted from a light source is divided into two paths, reference arm and measurement arm. The reflected lights from both arms recombine and make interference patterns, which is modulated by optical path difference, z . As the interference intensity, $I(z)$, is a sinusoidal signal, it can be simply expressed by

$$I(z) = I_0 (1 + \Gamma) \cos (2\pi/\lambda \cdot 2z) \quad (2-5)$$

where I_0 is background intensity, Γ is visibility, λ is wavelength, and z is optical path difference. The background intensity is proportional to the intensity of the light source, and visibility can be determined from degree of coherence of a light source. The brightest intensity of the interference pattern can be observed at $z = \lambda/4 \cdot n$ ($n=0, 2, 4, 6, \dots$), and the darkest intensity is at $z = \lambda/4 \cdot n$ ($n=1, 3, 5, \dots$). Because of its periodic pattern, the optical path difference can be determined within less than a half wavelength uniquely. In order to get over the 2π -ambiguity problem, the interference pattern should be counted continuously during the motion of the target mirror. This relative displacement measurement technique is one of the most precise metrological tools, and it can achieve measurement resolution of less than 1 nm with phase detection resolution of 1/1000, which is corresponding to $\lambda/2000$.

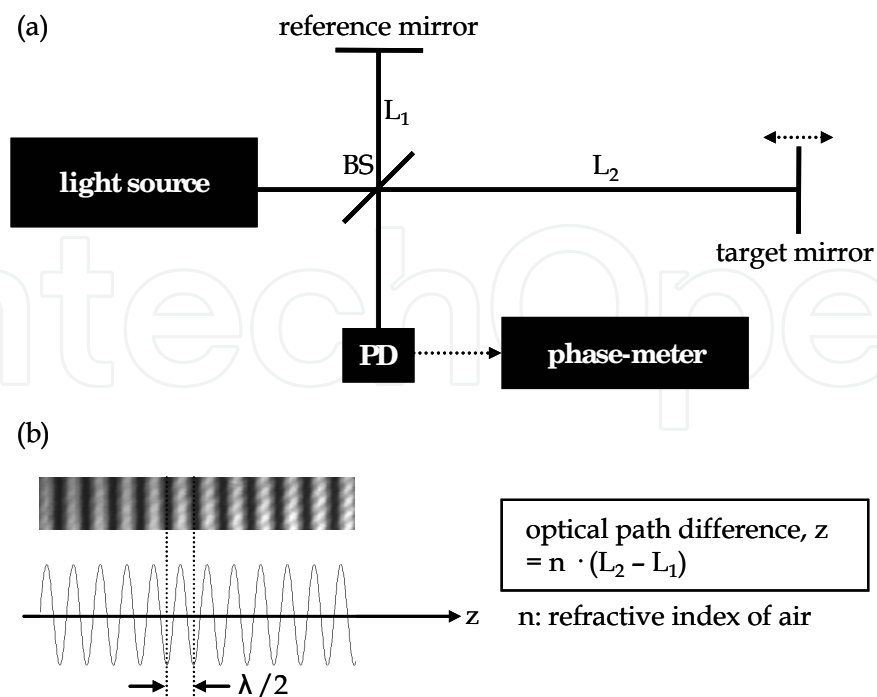


Fig. 2-11. Relative displacement measurement. (a) Michelson's interferometer setup, (b) Interference pattern caused by the optical path difference; BS (beam splitter), PD (photo-detector)

However, it has practical difficulties in the long-range measurement or large step measurement because the target mirror should be installed for translating from the initial position to the final position continuously without any interruption.

Multi-wavelength interferometer can solve this practical difficulty since it provides numbers of phase values obtained from several wavelengths. The distance, L , is given in the form of simultaneous equations as

$$L = \lambda_1/2 \cdot (m_1+f_1) = \lambda_2/2 \cdot (m_2+f_2) = \dots = \lambda_N/2 \cdot (m_N+f_N) \quad (2-6)$$

where the subscript N indicates the total number of individual wavelengths in use. As all m_i ($i=1,2,3,\dots,N$) should be positive integer numbers, a unique solution of L can be determined by solving equation (2-6) numerically in association with a proper estimation for the feasible range of L . In doing that, the required minimum number of wavelengths increases when the extent of the unknown range of L increases. As a general rule, four equations are found to be enough when a good assumption of L is available with an error of less than ± 1 mm.

The combined standard uncertainty of the measured distance, $u(L)$ comes from the uncertainty of air wavelength, $u(\lambda)$, and uncertainty for phase detection, $u(f)$. The combined standard uncertainty is given as

$$u(L) = [(u(\lambda)/\lambda)^2 L^2 + (\lambda \cdot u(f))^2]^{1/2} \quad (2-7)$$

The uncertainty of air wavelength, $u(\lambda)/\lambda$, comes from stability of the vacuum wavelength of the light source and uncertainty related to compensation of a refractive index of air. Commercialized laser for metrological use has a stability of vacuum wavelength of more than 10^{-8} . The uncertainty related to refractive index of air can be up to 10^{-7} in the typical environment controlled laboratory by monitoring the environment parameters such as temperature, relative humidity, pressure, etc. Since relative term in equation (2-7) is proportional to the distance, L , thus it can be neglected for short measurement range. For long-range measurement, this term will be dominant. However, for the measurement in the vacuum condition or in space, this term will be disappeared.

The uncertainty of phase detection, $u(f)$, is $\sim 1/100$ for commercialized phase-meter. The second term in the right side of equation (2-7) is proportional to the wavelength in use. Because the optical wavelength for optical interferometry is several hundreds nm, this term will be several nm. When the shorter wavelength is used or the electronics of phase-meter is improved, this term will be decreased.

Wavelength sweeping interferometer is also one of good candidates of absolute distance measurement, which can determine distance directly without any motions of a target mirror. Instead of moving the target mirror, wavelength of the light source will be swept continuously from λ_1 to λ_2 to obtain distance, L . During wavelength sweeping, changes of the interference pattern, Δm and Δf , are detected according to equation (2-8).

$$L = \lambda_1/2 \cdot (m_1+f_1) = \lambda_2/2 \cdot (m_1+\Delta m+f_1+\Delta f) \quad (2-8)$$

where Δm , Δf are changes in the integer part and the excess fraction part, respectively. After removing unknowns, m_1 and f_1 , length, L , can be expressed as equation (2-9) in terms of a synthetic wavelength, λ_s , simply.

$$L = \lambda_1\lambda_2/2 |\lambda_1-\lambda_2| \cdot (\Delta m+\Delta f) = \lambda_s/2 \cdot (\Delta m+\Delta f) \quad (2-9)$$

Since the synthetic wavelength, λ_s , is much longer than optical wavelengths, λ_1 and λ_2 , the phase unambiguity range can be extended. For example, when the wavelengths of λ_1 and λ_2 are 630 nm and 630.01 nm respectively, the synthetic wavelength becomes 39.690630 mm. Wavelength sweeping interferometer has advantages; it does not need multiple stabilized light sources and the initial estimation of L . However, the combined standard uncertainty of wavelength sweeping interferometer is worse than that of the multi-wavelength interferometer because of long synthetic wavelength, λ_s . The combined standard uncertainty can be derived as equation (2-10), which is similar to equation (2-7). The length dependent term of equation (2-10) is related to the stability of synthetic wavelength, which is $\sim 10^{-6}$. The second term of the right side related to the phase detection will be dominant even if the uncertainty of phase detection, $u(f)$, is extremely small due to the long synthetic wavelength. For example, this term will be approximately 0.4 mm when the synthetic wavelength is 40 mm and the uncertainty of phase detection is 1/100.

$$u(L) = [(u(\lambda_s)/\lambda_s)^2 L^2 + (\lambda_s \cdot u(f))^2]^{1/2} \quad (2-10)$$

3. Precision dimensional metrology using the optical frequency generators

3.1 Precision length calibration of gauge blocks

Gauge block is one of the widely-used length standards in industry. In order to retain a traceability chain from the definition of metre, gauge blocks should be calibrated based on the well-defined wavelengths. For this task, lots of national metrology institutes have been installed and operated optical interferometer systems for gauge block calibration.

Figure 3-1 shows gauge block calibration system installed in KRISS (Korea research institute of standards and science). The system consists of three major parts; light sources, interferometer part, and environment monitoring part. Light source part contains three different lasers, which are stabilized HeNe laser (633 nm), frequency doubled Nd:YAG laser (532 nm), and Rb-stabilized laser (532 nm). The light in use is selected by mechanical shutters, and then is delivered to the interferometer part via an optical fiber. The delivered light is collimated and divided into two paths; one goes to the reference mirror and the other goes to the gauge block attached to the platen. The reflected lights interfere with each other, and are observed by the CCD camera. In order to compensate the refractive index of air using Edlen's formula, environment parameters such as temperature, pressure, relative humidity and CO₂ contents in the air are monitored. And the interferometer part is isolated by thermal insulators at standard temperature of 20 °C.

Optical frequency generator with a working laser can be a newly developed light source for gauge block calibration. The wavelength generation range of the optical frequency generator is from 765 nm to 781 nm. The coarse tuning using DC-motor attached on the mirror of the extra cavity has the resolution of 0.02 nm with the maximum speed of 8 nm/s. And fine tuning range using PZT attached on the mirror is 0.15 nm (75 GHz) with control bandwidth of 2 kHz. The optical power of the optical frequency generator is about 10 mW, which is sufficient for length metrology. The linewidth of the working laser is 300 kHz at 50ms, which allows the coherence length of more than 1 km. For gauge block calibration the optical frequency generator produces four different wavelengths (776.99983 nm, 777.99925 nm, 779.99727 nm, and 781.00002 nm) instead of using several stabilized light sources such as HeNe laser, Nd:YAG laser, etc. Since this concept gives the traceability to the time standard directly, the direct connection between length and time standards can be realized.

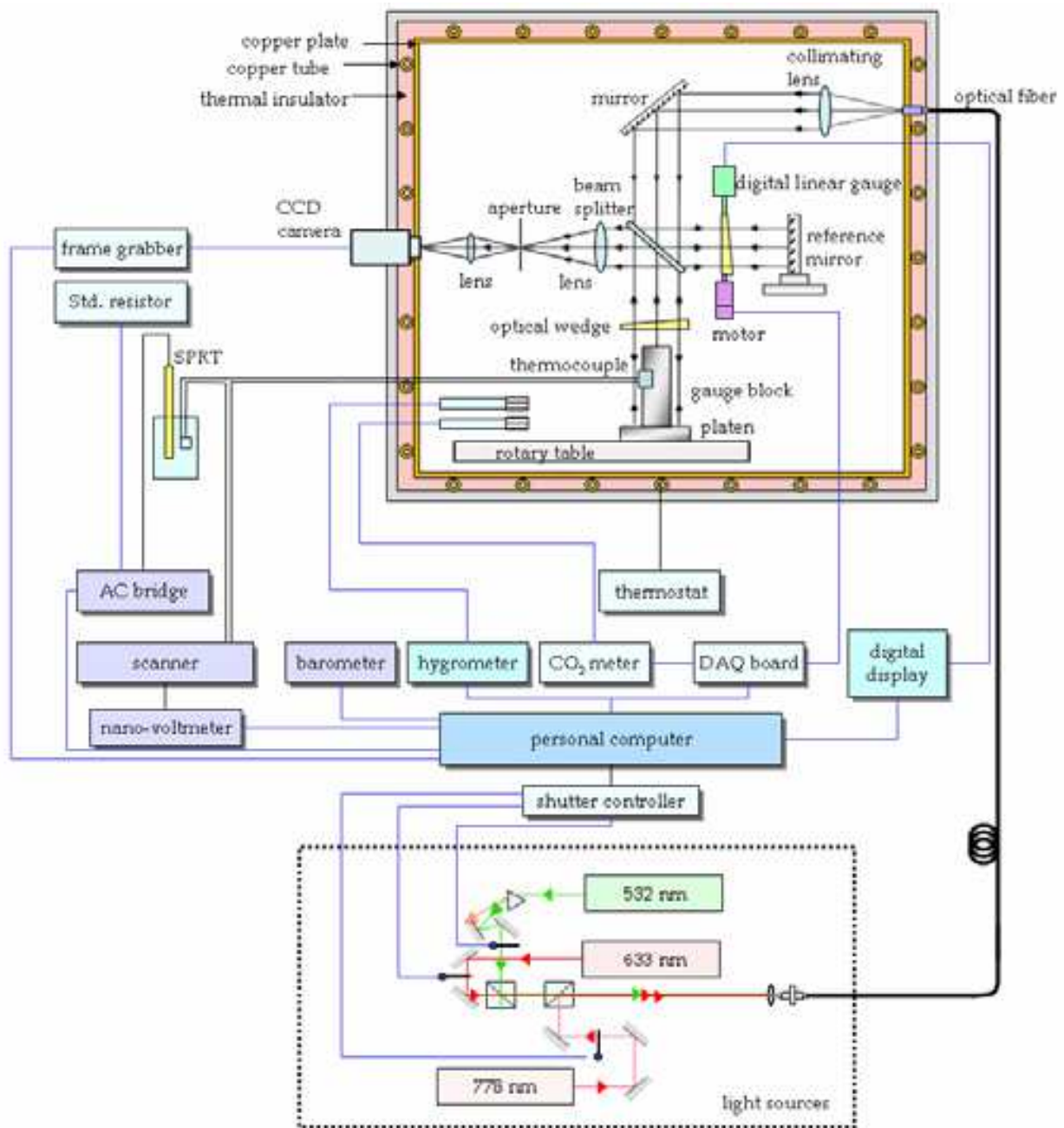


Fig. 3-1. Layout of gauge block calibration system in KRISS

Figure 3-2 shows the optical layout of the gauge block calibration system based on the optical frequency generator. The interferometer setup is basically same as the previous gauge block calibration system in KRISS. The light emitted by optical frequency generator is collimated by a double-let lens with the diameter of 50 mm, and then goes to the plate type beam splitter through a tuning mirror. The separated lights propagate both a gauge block attached on a base plate and reference mirror, and then reflect. The interference pattern can be observed by 2D CCD camera. The environmental parameters (pressure, temperature, relative humidity, and CO₂ contents in the air) are monitored to compensate the refractive index of the air during the measurements.

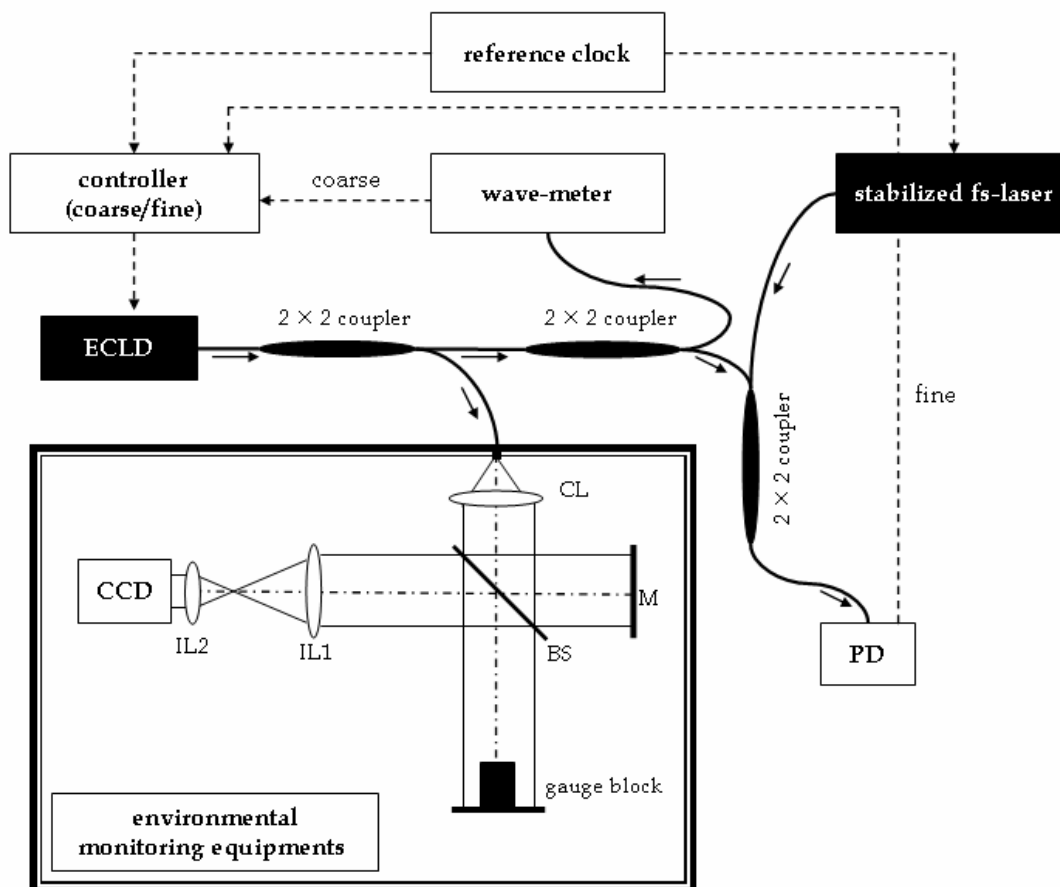


Fig. 3-2. Optical layout of the gauge block calibration system based on the optical frequency generator; CL (collimation lens), M (mirror), BS (beam splitter), IL (imaging lens), PD (photo-detector), ECLD (external cavity laser diode)

The length of the gauge block can be determined by phase difference between top surface of the gauge block and the base plate. Fourier-transform method was adopted for phase determination. The three different lines are chosen; one (G) is at the center of the top surface of the gauge block and the other lines (B_a and B_b) are at the base plate with same offset from the chosen line at the top surface of the gauge block. In order to eliminate the DC component, the slopes of lines are removed by least square method. And then these are Fourier-transformed with Hanning window after zero-padding to improve the resolution in the spectral domain. The initial phase of each line can be extracted at the peak of the amplitude in the spectral domain. The phase of the base plate can be determined by averaging the phase values of B_a and B_b to eliminate the tilting effect of the gauge block and the base plate. Excess fraction parts in equation (2-6) for each wavelength can be given by phase difference between the phase at the center of top surface of the gauge block (Φ_G) and the average phase of the base plate. Figure 3-3 shows the overall calculation procedure of the excess fraction part based on Fourier-transform method.

The measurement result of 25 mm gauge block is summarized in Table 3-1. The excess fraction parts were obtained by Fourier-transform method from interference patterns as described before. To cancel out the random vibration effect, 20 interference patterns were

captured repeatedly at each wavelength. The standard deviation of the excess fraction was less than 5/100. The mean value of the calculated length of the gauge block was 24.999890 mm when the refractive index of air and temperature of gauge block were corrected.

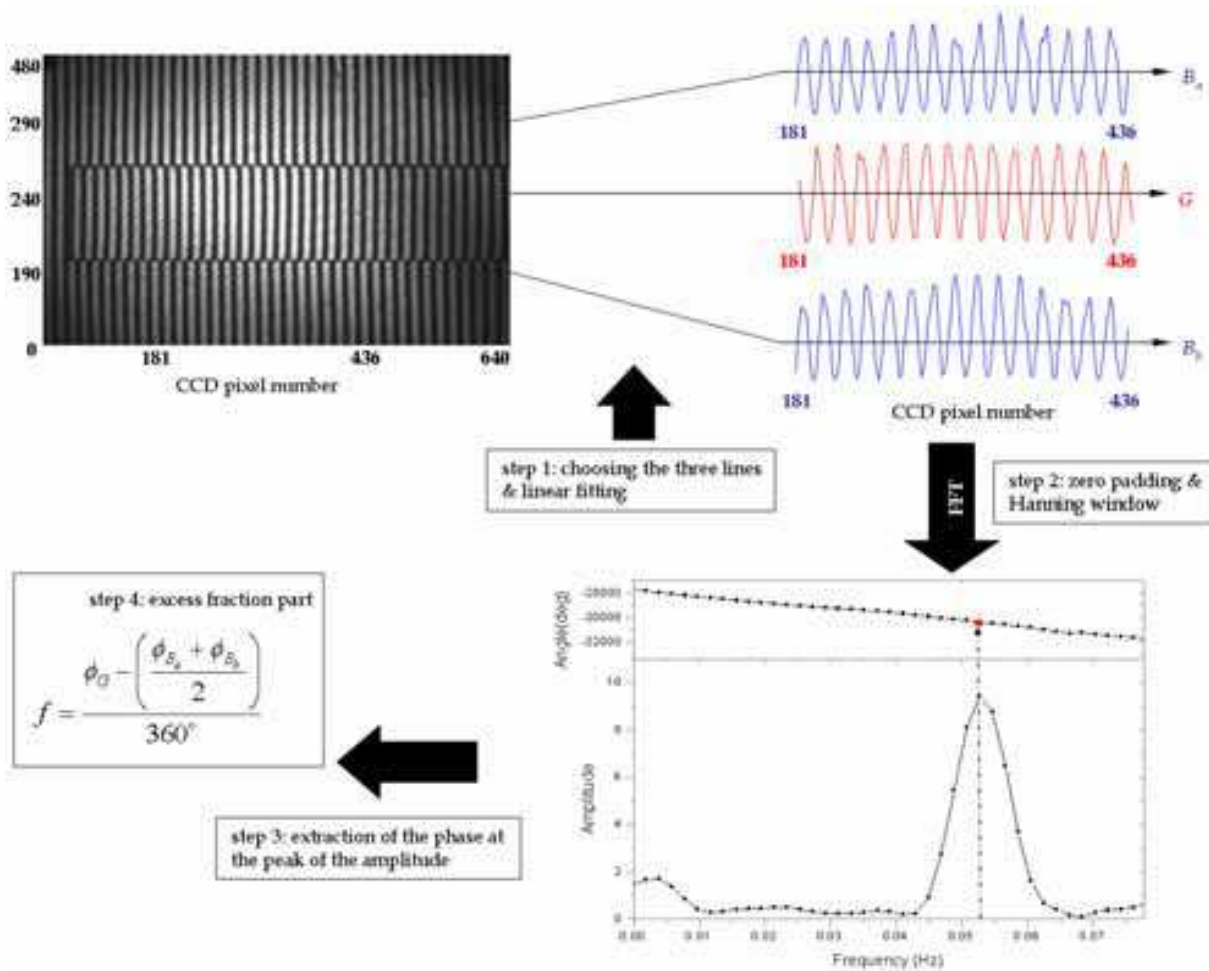


Fig. 3-3. Calculation procedure of the excess fraction part based on Fourier-transform method

State	Measured and computed data			
	1	2	3	4
Vacuum wavelength (nm)	776.99983	777.99925	779.99727	781.00002
Excess fraction, f	0.9483	0.2591	0.5773	0.2430
Deviation of f	0.0010	0.0014	0.0010	0.0047
Integer part, m	64366	64284	64119	64037
Absolute distance, L (nm)	24999890.2	24999888.9	24999890.2	24999888.7
Stability of measured excess fraction		0.0035		
Thermal expansion coefficient of gauge block		$8.4 \times 10^{-6} / K$		
Refractive index of air		1.00027050		

Absolute distance, L, finally determined by averaging the computed values: 24.999890 mm
(The refractive index of air and temperature of gauge block are corrected.)

Table 3-1. Measurement result of 25 mm gauge block.

The length of gauge blocks based on the optical interferometry, L , can be expressed as

$$L = \text{mean}[\lambda_i/2 \cdot (m_i + f_i)] - \text{mean}[L_0 \cdot (n_i - 1)] - L_0\alpha(T_{\text{GB}} - 20) + L_\Phi + L_W + L_E + L_G \quad (3-1)$$

$$= L_{\text{fit}} + L_n + L_T + L_\Phi + L_W + L_E + L_G$$

where, i is integer number ($i=1, 2, 3, \dots, N$), N indicates the total number of individual wavelengths in use, $\text{mean}[A_i]$ is the mean value of A_i , L_0 is nominal value of the gauge block, n is refractive index of air, α is thermal expansion coefficient of the gauge block, T_{GB} is temperature of the gauge block, L_{fit} is the measured length based on the optical interferometry, L_n , L_T , L_Φ , L_W , L_E , and L_G are the lengths corresponded to the compensation of refractive index of air, correction of thermal expansion to the standard temperature of 20 °C, phase compensation for surface roughness of the gauge block and the base plate, wringing process, optical components errors, and geometrical errors such as parallelism, flatness, respectively.

The uncertainty of determination of the excess fractions at four difference wavelengths (777 nm, 778 nm, 780 nm, and 781 nm) is 0.02, which is caused by repeatability of phase detection and stability of the measured excess fraction, 0.0035. And the uncertainty of the wavelengths in use is 1.9×10^{-10} , which comes from the frequency stabilities of the repetition rate, carrier-offset frequency, and beat note between the optical comb and a working laser. Therefore, the uncertainty of the gauge block calibration interferometer becomes as

$$u(L_{\text{fit}}) = [(7.8 \text{ nm})^2 + (1.9 \times 10^{-10} \cdot L_0)^2]^{1/2} \quad (3-2)$$

The air wavelength can be obtained by dividing the vacuum wavelength into the refractive index of air. The refractive index of air can be determined by updated Edlen's formula with the environmental parameters of temperature, pressure, relative humidity, and CO_2 contents of air. The uncertainty of measuring environmental parameters comes from equipment measuring accuracy and deviation of parameters during the experiments. The uncertainty of temperature is 5.2 mK when the deviation of temperature is 1.5 mK with measurement uncertainty of thermometer, 5 mK ($k=1$). The uncertainty of relative humidity is given as 1.0 % R.H. at 20 % R.H. caused by equipment accuracy of 1.0 % R.H. and deviation of 0.01 % R.H. The uncertainty of pressure is 3.0 Pa at 1 atm when the deviation is 0.45 Pa with measurement accuracy of a manometer, ± 0.003 %. The uncertainty of CO_2 contents in air is estimated 10.0 ppm at 450 ppm caused by equipment accuracy of ± 1 % and deviation of 5.5 ppm. The uncertainty of update Edlen formula itself is 10^{-8} . These uncertainty factors give the uncertainty of air wavelength as

$$u(L_n) = 1.4 \times 10^{-8} \cdot L_0 \quad (3-3)$$

Since the length of gauge block is defined at the temperature of 20 °C, the thermal expansion of the gauge block caused by temperature difference should be compensated. The material of gauge block and base plate is chrome carbide, which has the thermal expansion coefficient of 8.4×10^{-6} /K. The uncertainty of thermal expansion coefficient is $1.0/\sqrt{3} \times 10^{-6}$ /K, and the uncertainty of the temperature of the gauge block is 15 mK. The uncertainty of the compensation of thermal expansion could be expressed as

$$u(L_T) = 1.3 \times 10^{-7} \cdot L_0 \quad (3-4)$$

The uncertainty of phase compensation for surface roughness of the gauge block and the base plate comes from the optical constant differences caused by different materials and surface roughness of gauge block and base plate. The term related to optical constant differences can be ignored by adopting the same material for the gauge block and the base plate. The uncertainty of surface roughness is estimated 5 nm by mechanical or optical profilers.

The uncertainty of wringing effect is 6.9 nm, which can be determined by wringing the same gauge block on the base plate repeatedly. The uncertainty of optical components can be estimated by wave-front errors of each components, $\lambda/10 \sim \lambda/20$. However, it's very difficult to extract optical system error from the each, which can be determined by measuring amount of bending of interference patterns generated by the installed Twyman-Green interferometer with two flat mirrors. It is estimated as $\lambda/15$ within 2/5 of full measurement area, which is only used for this calibration task. Therefore, the uncertainty of optical

Uncertainty sources	Contributions	Numerical values for $L_0=25$ mm
Gauge block interferometer	$[(7.8 \text{ nm})^2 + (1.9 \times 10^{-10} \cdot L_0)^2]^{1/2}$	7.8 nm
Excess fraction	0.02	
Wavelength in use	1.9×10^{-10}	
Repetition rate	1.3×10^{-12}	
Carrier-offset frequency	8.1×10^{-13}	
Beat note	1.9×10^{-10}	
Estimating the refractive index of air	$1.4 \times 10^{-8} L_0$	0.4 nm
Air temperature	5.2 mK	
Air pressure	3 Pa	
Air humidity	0.6 % R.H.	
CO ₂ content in air	6.0 ppm	
Edlen's formula	10^{-8}	
Thermal expansion of gauge block	$1.3 \times 10^{-7} L_0$	3.3 nm
Thermal expansion coefficient	$5.8 \times 10^{-7} / ^\circ\text{C}$	
Surface temperature of gauge block	15 mK	
Wave-front error of the optical components of the gauge block interferometer	12 nm	12 nm
Wringing of gauge block	6.9 nm	6.9 nm
Surface roughness of gauge block	5.0 nm	5.0 nm

* L_0 denotes the nominal length of a gauge block whose length is given in meter.

Table 3-2. Uncertainty evaluation of absolute calibration of gauge blocks.

components becomes 12 nm. The uncertainty of geometrical errors is 0.6 nm, which can be given according to ISO defined grade of gauge blocks.

Table 3-2 shows the summary of the uncertainty evaluation of the absolute calibration of gauge blocks. The combined standard uncertainty is 17 nm ($k=1$) for the 25 mm gauge block.

This research was a meaningful work because it was a first realization of length and time connection. Even if the standard was well established in national metrological institutes, the traceability chain should be coupled well for maintaining the nation's industrial quality. Therefore, the calibration of gauge block is an important task to keep the traceability chain from the standard because the gauge block is one of the practical length standards, and widely used in the industry. As the time standard has the higher stability and uncertainty, the dimensional metrology will have better uncertainty by linking length to time standards.

3.2 Absolute distance measurement

Absolute distance measurement can determine the length with a single operation based on optical interferometry. Based on the two absolute distance measurement techniques described in section 2.3, multi-wavelength interferometer and wavelength sweeping interferometer, the distance can be obtained with the optical frequency generator; Four different wavelengths, λ_1 , λ_2 , λ_3 and λ_4 , are chosen as 780.206901 nm, 780.203668 nm, 779.953524 nm and 770.204349 nm, respectively for multi-wavelength interferometer principle, and the wavelength between λ_1 and λ_2 is scanned continuously for wavelength sweeping interferometer as shown in figure 3-4. During the wavelength scanning for rough estimation of the distance, the change of phase in terms of the integer part and the excess fraction part in equation (2-9), Δm and Δf , are 13 and -0.06940, respectively. That leads to an estimation of the distance as 1195.205502 nm along with a synthetic wavelength, λ_s , of 184.853 nm. The optical heterodyne technique is adopted for real-time phase detection, and it is realized that the optical frequency is slightly shifted by the two acousto-optic modulators, AOM1 and AOM2, in series as shown in figure 3-5. The avalanche photo-detector, APD1, monitors the reference signal as $A \cdot \cos[2\pi\Delta f \cdot t]$, and the other avalanche photo-detector, APD2, obtains the measurement signal as $B \cdot \cos[2\pi\Delta f \cdot t + \Phi]$, where A and B denote amplitude, Δf is frequency difference caused by two AOMs, phase shift, Φ , represents $4\pi f \cdot L$. The commercialized phase-meter can detect the phase shift, Φ , with the bandwidth of more than 1 kHz. From the value of phase shift, the distance, L can be extracted with the uncertainty of phase-meter accuracy, $0.0016 \cdot \lambda_s/2$. And the uncertainty of the measured excess fractions is $0.0012 \cdot \lambda_s/2$. Therefore, the uncertainty of the phase detection is estimated as 258.8 μm .

The uncertainty of the synthetic wavelength comes from the uncertainty of wavelength in use. It is evaluated as $2.0 \times 10^{-6} \cdot L$, which leads 2.4 μm at the distance of 1.195 m. And the uncertainty for refractive index of air is only 17 nm, which can be determined by $1.4 \times 10^{-8} \cdot L$ at $L=1.2$ m. Therefore, the estimation distance of 1195.205502 nm has the measurement uncertainty of 258.8 μm , which can be calculated according to the equation (2-10). The uncertainty of phase detection is the most contributed uncertainty component in this measurement. It is important note that the estimation value is a good assumption for multi-wavelength interferometer.

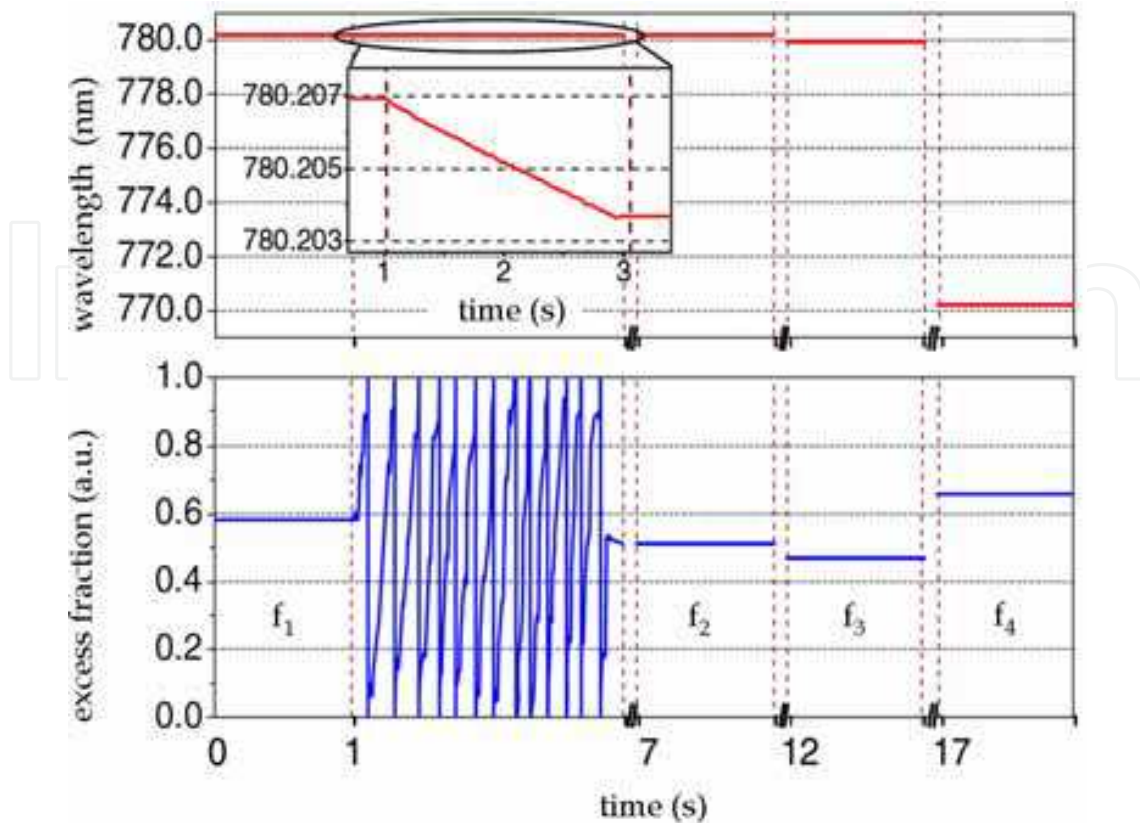


Fig. 3-4. Wavelength generation profile and the changes of phase in terms of excess fraction for the absolute distance measurement.

State	Measured and computed data			
	1	2	3	4
Vacuum wavelength (nm)	780.206961	780.203668	779.953524	770.204349
Refractive index of air	1.000263346	1.000263345	1.000263347	1.000263410
Air wavelength (nm)	780.001551	779.998260	779.748180	770.001523
Excess fraction, f	0.5817	0.5123	0.4688	0.6578
Deviation of f	0.0007	0.0002	0.0011	0.0005
Integer part, m	3064834	3064847	3065830	3104637
Absolute distance, L (nm)	1195.287863	1195.287863	1195.287865	1195.287862

Initial estimation of L by means of sweeping wavelength from state 1 to 2: 1195.205502 mm

Absolute distance, L , finally determined by averaging the computed values: 1195.287863 mm

Table 3-3. summary of experimental data for the absolute distance of ~ 1.2 m

The uncertainty of the optical frequency generator comes from the uncertainties of repetition rate, carrier-offset frequency, and beat note as mentioned in the section 3.1. However, the uncertainty is improved by the modified electric control loop with high-performance filters. It is estimated as $5.9 \times 10^{-12} \cdot L$, which is 0.01 nm at $L=1.195$ m. The uncertainty of refractive

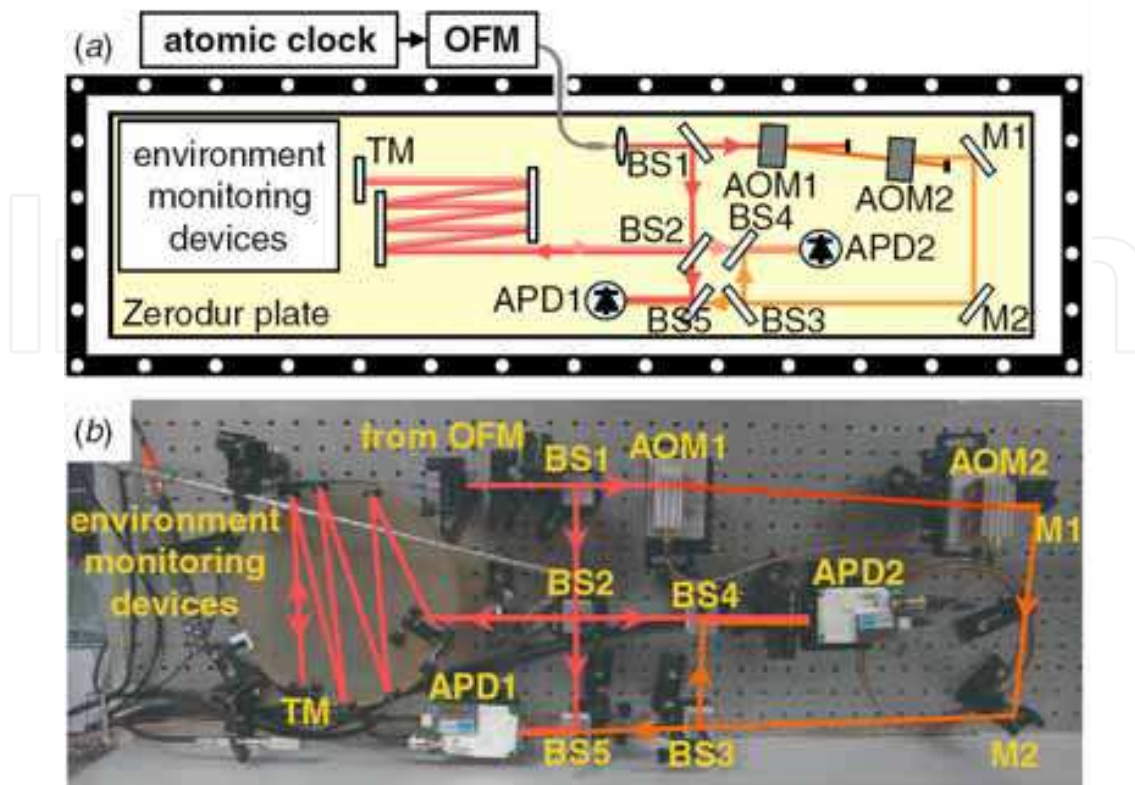


Fig. 3-5. Interferometer setup for absolute distance measurement. (a) schematic of the interferometer, (b) photo of the interferometer; AOM(acousto-optic modulator), APD(avalanche photo-detector), BS(bean splitter), M(mirror), TM(termination mirror)

index of air is same as the previous task, which is given as 17.1 nm at $L=1.195$ m. The uncertainty of the multi-wavelength interferometer comes from the uncertainties of phase-meter accuracy, measured excess fractions, and the exact fraction method. It can be estimated as $0.0061 \cdot \lambda/2$, which is 2.3 nm. The combined standard uncertainty can be expressed as

$$u(L) = [(2.3 \text{ nm})^2 + (1.4 \times 10^{-8} \cdot L)^2]^{1/2} \quad (3-5)$$

At the measured distance of ~ 1.195 m, the combined standard uncertainty is 17.1 nm ($k=1$). Table 3-4 shows the uncertainty evaluation of absolute length measurement based on the optical frequency generator.

This absolute distance measurement has various applications; one is for precision positioning of space fleet. Several satellites make specific arrangements for obtaining large aperture, which gives high-quality images of the universe. The missions are for finding earth-like planets, discovering the fundamentals of the creation, and detecting the gravitational waves. Since this operation will be done in space, the uncertainty of the refractive index of air, the most dominant uncertainty, can be eliminated. The combined standard uncertainty for the precision positioning in space is proportional to the measuring distance, L , simply. For example, when the distance between satellites is 1 km, the combined

standard uncertainty is estimated only as 6.4 nm according to the table 3-4. The other is for positioning and control of ultra-precision stages in the field of semi-conductor and flat-panel display. The travel of these stages is several meters in the well-stabilized environmental conditions. Generally the relative displacement measurement technique has been used for these applications, but it has drawbacks; since it can not give the absolute values, the stage should be moved from a reference point continuously to obtain the absolute coordinates. Because it is occurred some drifts due to the environment variation and mis-reading of interference signals, homing (setting a reference point) should be done periodically. Absolute distance measurement will be a good alternative measurement solution for these applications.

Uncertainty sources	Contributions	Numerical values for L= \sim 1.195 m
Optical frequency generator	$5.9 \times 10^{-12} L$	0.01 nm
Repetition rate	1.3×10^{-12}	
Carrier-offset frequency	2.2×10^{-12}	
Beat note	5.8×10^{-12}	
Estimating the refractive index of air	$1.4 \times 10^{-8} L$	17.1 nm
Air temperature	5.2 mK	
Air pressure	3 Pa	
Air humidity	0.6 % R.H.	
CO ₂ content in air	6.0 ppm	
Edlen's formula	10^{-8}	
Multi-wavelength interferometer	$0.0061 \times \lambda/2$	2.3 nm
Phase-meter accuracy	$0.0016 \times \lambda/2$	
Measured excess fractions	$0.0012 \times \lambda/2$	
Multi-wavelength algorithm	$0.0058 \times \lambda/2$	
Combined standard uncertainty ($k=1$)	$[(2.3 \text{ nm})^2 + (1.4 \times 10^{-8} L)^2]^{1/2}$	17.1 nm

Table 3-4. Uncertainty evaluation of absolute distance measurement

4. Summary and future works

Dimensional metrology has a long history from the ancient times. The long sticks or bars have been used with precision scales on that for measuring length. In the 18th century the light emitted from lamps was suggested and realized as a tool for precision dimensional metrology by using interference phenomenon. In 1960s the advent of laser opened a new way for precision length and profile measurement techniques, which leads today's optical interferometry using long coherence length. Recently the fs pulse laser has been in spotlight because of its short pulse duration and the wide spectral bandwidth, which allows precision

optical frequency metrology and spectroscopy with the traceability to the frequency standard.

In this chapter, the fs pulse laser was adopted as a light source for precision dimensional metrology. The optical comb of the fs pulse laser was acted as scales in the optical frequency regime. Based on that, the two types of optical frequency generators, which could produce a desired single wavelength with high stability, were suggested and realized. One was constructed with a working laser, which could tune the wavelength within the range of 20 nm. Due to low control rate caused by mechanical resonance, it had degradation in terms of wavelength stability and line-width. The other was based on direct extraction of a single mode from the optical comb with the help of optical filtering components, a diffraction grating-optical fiber pairs and scanning Fabry-Perot etalon. However, the extracted mode should be amplified for dimensional measurement because it was too weak to use. The injection locking technique was adopted for this amplification process. This type of the optical frequency generator could maintain the wavelength stability, which was same as the reference clock. If the several diode lasers with different emission wavelengths will be locked to the optical comb at the same time, the distance can be measured in real-time by shortening the wavelength tuning procedure.

Absolute distance measurement can determine the distance with a single operation without 2π ambiguity problem. It could be realized by using the optical frequency generator, which could produce individual wavelengths and scan the wavelength smoothly. By adopting the optical frequency generator as a light source the absolute length calibration of gauge blocks could be realized with the combined standard uncertainty of 17 nm for 25 mm gauge blocks. Four individual wavelengths were chosen for multi-wavelength interferometer, the phases at each wavelength were obtained by Fourier-transform method. This standard work gave the direct coupling between length and time because the optical comb of a fs pulse laser was stabilized to the atomic reference clock, frequency standard. Now KRISS is expanding this scheme to the long range gauge block of more than 1 m.

The absolute distance of 1.195 m was measured using the optical frequency generator. To obtain the estimated value of the distance, wavelength sweeping interferometer principle was applied. With the estimated value, the absolute distance was determined by measured phases at four different wavelengths. The phases were obtained by optical heterodyne technique in real-time. The combined standard uncertainty of the measured distance of 1.195 m was 17.1 nm. In this case, the combined standard uncertainty will be decreased dramatically in the vacuum condition because the most dominant uncertainty was uncertainty of refractive index of air. That means it will a good solution for satellite fleets for space missions or precision stages operating in the vacuum. And a fs pulse laser based on optical fiber allows more simple and reliable measurements in industry because of its easy handling and low cost.

5. Acknowledgements

These research works were accomplished at KAIST (principal investigator: Prof. Seung-Woo Kim, swk@kaist.ac.kr). Now Dr. Jonghan Jin is working as a senior researcher at Centre for Length and Time, Division of Physical Metrology, Korea Research Institute of Standards and Science (KRISS), and the present e-mail address is jonghan@kriss.re.kr.

6. References

- Jin, J.; Kim, Y. -J.; Kim, Y.; Kim, S. -W. & Kang, C. -S. (2006) Absolute length calibration of gauge blocks using the optical comb of a femtosecond pulse laser, *Optics Express*, Vol. 14, No. 13, pp. 5568-5974, ISSN 1094-4087
- Jin, J.; Kim, Y. -J.; Kim, Y. & Kim, S. -W. (2007) Absolute distance measurement using the optical comb of a femtosecond pulse laser, *International Journal of Precision Engineering and Manufacturing*, Vol. 8, No. 7, pp. 22-26, ISSN 1229-8557
- Kim, Y. -J.; Jin, J.; Kim, Y. ; Hyun, S. & Kim, S. -W. (2008) A wide-range optical frequency generator based on the frequency comb of a femtosecond laser, *Optics Express*, Vol. 16, No. 1, pp. 258-264, ISSN 1094-4087
- Hyun, S.; Kim, Y. -J.; Kim, Y. ; Jin, J. & Kim, S. -W. (2009) Absolute length measurement with the frequency comb of a femtosecond laser, *Measurement Science and Technology*, Vol. 20, pp. 095302-1-6, ISSN 0957-0233
- Minoshima, K. & Matsumoto, H. (2000) High-accuracy measurement of 240-m distance in an optical tunnel by use of a compact femtosecond laser, *Applied Optics*, Vol. 39, No. 30, pp. 5512-5517, ISSN 0003-6935
- Yamaoka, Y.; Minoshima, K. & Matsumoto, H. (2002) Direct measurement of the group refractive index of air with interferometry between adjacent femtosecond pulses, *Applied Optics*, Vol. 41, No. 21, pp. 4318-4324, ISSN 0003-6935
- Bitou, Y.; Schibli, T. R.; Minoshima, K. (2006) Accurate wide-range displacement measurement using tunable diode laser and optical frequency comb generator, *Optics Express*, Vol. 14, No. 2, pp. 644-654, ISSN 1094-4087
- Schibli, T. R.; Minoshima, K.; Bitou, Y.; Hong, F. -L.; Bitou, Y.; Onae, A. & Matsumoto, H. (2006) Displacement metrology with sub-pm resolution in air based on a fs-comb wavelength synthesizer, *Optics Express*, Vol. 14, No. 13, pp.5984-5993, ISSN 1094-4087
- Bitou, Y. & Seta K. (2000) Gauge block measurement using a wavelength scanning interferometer, *Japanese Journal of Applied Physics*, Vol. 39, pp. 6084-6088, ISSN 0021-4922
- Schibli, T. R.; Minoshima, K.; Hong, F. -L.; Inaba, H.; Onae, A.; Matsumoto, H.; Hartl, I.; Fermann, M. E. (2004) Frequency metrology with a turnkey all-fiber system, *Optics Letters*, Vol. 29, No. 21, pp.2267-2469, ISSN 0146-9592
- Lay, O. P.; Dubovitsky, S.; Peters, R. D. & Burger, J. P (2003) MSTAR: a submicrometer absolute metrology system, *Optics Letter*, Vol. 28, pp. 890-892, ISSN 0146-9592
- Walsh, C. J. (1987) Measurement of absolute distances to 25 m by multiwavelength CO₂ laser interferometry, *Applied Optics*, Vol. 26, No. 9, pp. 1680-1687, ISSN 0003-6935
- Bien, F.; Camac, M.; Caulfield, H. J. & Ezekiel, S. (1981) Absolute distance measurements by variable wavelength interferometry, *Applied Optics*, Vol. 20, No. 3, pp. 400-403, ISSN 0003-6935
- Dändliker, R.; Thalmann, R. & Rregué (1988) Two-wavelength laser interferometry using super heterodyne detection, *Optics Letters*, Vol. 13, No. 5, pp. 339-341, ISSN 0146-9592

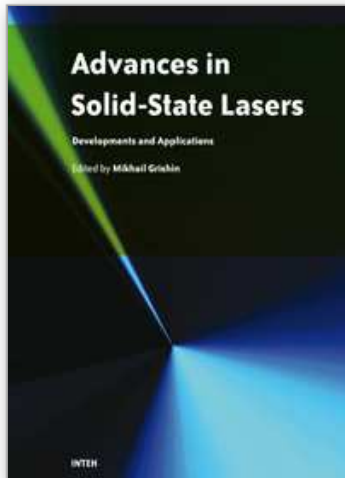
- Kubota, T.; Nara, M. & Yoshino, T. (1987) Interferometer for measuring displacement and distance, *Optics Letters*, Vol. 12, No. 5, pp. 310-312, ISSN 0146-9592
- Jost, J. D.; Hall, J. L. & Ye, J. (2002) Continuously tunable, precise, single frequency optical signal generator, *Optics Express*, Vol. 10, pp. 515-520, ISSN 1094-4087
- Birch, K. P. & Downs, M. J. (1993) An updated Edlen equation for the refractive index of air, *Metrologia*, Vol. 34, pp. 479-493, ISSN 0026-1394
- Schuhler, N.; Salvadé, Y.; Lévêque, S.; Dändliker, R & Holzwarth, R. (2006) Frequency-comb-referenced two-wavelength source for absolute distance measurement, *Optics Letters*, Vol. 31, No. 21, pp. 3101-3103, ISSN 0146-9592
- Slavadé, Y.; Schuhler, N.; Lévêque, S. & Floch, S. L. (2008) High-accuracy absolute distance measurement using frequency comb referenced multiwavelength source, *Applied Optics*, Vol. 47, No. 14, pp. 2715-2720, ISSN 0003-6935
- Coddington, I; Swann, W. C.; Nenadovic, L. & Newbury, N. R. (2009) Rapid and precise absolute distance measurement at long range, *Nature Photonics*, Vol. 3, pp. 351-356, ISSN 1749-4885
- Jin, J.; Kim, Y. -J.; Kim, Y. ; Hyun, S. & Kim, S. -W. (2008) Absolute distance measurement using the frequency comb of a femtosecond pulse laser, *Proceedings of the European Society of Precision Engineering and Nanotechnology (EUSPEN) International conference*, O7.2, Zurich, 05/2008, EUSPEN, Cranfield
- Jin, J.; Kim, Y. -J.; Kim, Y. ; Hyun, S. & Kim, S. -W. (2007) Precision length metrology using and optical frequency generator, *Proceedings of the Asian Society of Precision Engineering and Nanotechnology (ASPEN) 2007*, pp. 39-41, Kwangju, 11/2007, KSPE, Seoul (invited)
- Jin, J.; Kim, Y. -J.; Kim, Y. ; Hyun, S. & Kim, S. -W. (2007) Precision length metrology using and optical frequency synthesizer, *Proceedings of the Conference on Laser and Electro-Optics-Pacific Rim (CLEO-PR)*, pp. 1443-1444, Seoul, 08/2007, OSA, Seoul (invited)
- Jin, J.; Kim, Y. -J.; Kim, Y. & Kim, S. -W. (2006) Absolute length metrology using a femtosecond pulse laser, *Proceedings of the 2nd International Conference on Positioning Technology*, pp. 119-121, Daejeon, 10/2006, KSPE, Seoul
- Jin, J.; Kim, Y. -J.; Kim, Y.; Kim, S. -W. & Kang, C. -S (2006) Absolute length calibration of gauge blocks using optical comb of a femtosecond pulse laser, *Proceedings of SPIE Optics & Photonics*, pp. 6292O-1, San-diego, 08/2006, SPIE, Bellingham
- Jin, J.; Kim, Y. -J.; Kim, Y.; Kim, S. -W. & Kang, C. -S (2006) Absolute length calibration of gauge blocks using optical comb of a femtosecond pulse laser, *Proceedings of the European Society of Precision Engineering and Nanotechnology (EUSPEN) International conference*, pp. 410-414, Baden, 05/2006, EUSPEN, Cranfield
- Kim, S. -W.; Oh, J. S.; Jin, J.; Joo, K. N. & Kim, Y. -J. (2005) New precision dimensional metrology using femtosecond pulse lasers, *Proceedings of the European Society of Precision Engineering and Nanotechnology (EUSPEN) International conference*, pp. 135-138, Montpellier, 05/2005, EUSPEN, Cranfield
- Kim, S. -W.; Joo, K. N.; Jin, J. & Kim, Y. -J. (2005) Absolute distance measurement using femtosecond laser, *Proceedings of SPIE*, pp. 58580N-1-8, Munich, 06/2005, SPIE, Bellingham

Ye, J. & Cundiff, S. T. (2005). *Femtosecond optical frequency comb: Principle, operation, and applications*, Springer, ISBN 0-387-23790-9, New York

Rullière, C. (1998). *Femtosecond laser pulses; Principles and experiments*, Springer, ISBN 3-540-63663-3, Berlin Heidelberg

IntechOpen

IntechOpen



Advances in Solid State Lasers Development and Applications

Edited by Mikhail Grishin

ISBN 978-953-7619-80-0

Hard cover, 630 pages

Publisher InTech

Published online 01, February, 2010

Published in print edition February, 2010

Invention of the solid-state laser has initiated the beginning of the laser era. Performance of solid-state lasers improved amazingly during five decades. Nowadays, solid-state lasers remain one of the most rapidly developing branches of laser science and become an increasingly important tool for modern technology. This book represents a selection of chapters exhibiting various investigation directions in the field of solid-state lasers and the cutting edge of related applications. The materials are contributed by leading researchers and each chapter represents a comprehensive study reflecting advances in modern laser physics. Considered topics are intended to meet the needs of both specialists in laser system design and those who use laser techniques in fundamental science and applied research. This book is the result of efforts of experts from different countries. I would like to acknowledge the authors for their contribution to the book. I also wish to acknowledge Vedran Kordic for indispensable technical assistance in the book preparation and publishing.

How to reference

In order to correctly reference this scholarly work, feel free to copy and paste the following:

Jonghan Jin and Seung-Woo Kim (2010). Precision Dimensional Metrology Based on a Femtosecond Pulse Laser, *Advances in Solid State Lasers Development and Applications*, Mikhail Grishin (Ed.), ISBN: 978-953-7619-80-0, InTech, Available from: <http://www.intechopen.com/books/advances-in-solid-state-lasers-development-and-applications/precision-dimensional-metrology-based-on-a-femtosecond-pulse-laser>

INTECH
open science | open minds

InTech Europe

University Campus STeP Ri
Slavka Krautzeka 83/A
51000 Rijeka, Croatia
Phone: +385 (51) 770 447
Fax: +385 (51) 686 166
www.intechopen.com

InTech China

Unit 405, Office Block, Hotel Equatorial Shanghai
No.65, Yan An Road (West), Shanghai, 200040, China
中国上海市延安西路65号上海国际贵都大饭店办公楼405单元
Phone: +86-21-62489820
Fax: +86-21-62489821

© 2010 The Author(s). Licensee IntechOpen. This chapter is distributed under the terms of the [Creative Commons Attribution-NonCommercial-ShareAlike-3.0 License](#), which permits use, distribution and reproduction for non-commercial purposes, provided the original is properly cited and derivative works building on this content are distributed under the same license.

IntechOpen

IntechOpen